Calculation of the Cross Power Spectral Density for Pulse Mode Detectors

A. Talamo,[a] Y. Gohar,[a] T. Yamamoto,[b] M. Yamanaka,[b] C. H. Pyeon[b]

[a)]Argonne National Laboratory, 9700 South Cass Avenue, Argonne, IL 60439, USA
[b)]Kyoto University, Kumatori-cho, Sennan-gun, 590-0494, Osaka, Japan

[*]alby@anl.gov

INTRODUCTION

This work introduces a novel methodology to calculate the cross power spectral density for detectors operating in pulse mode. In this operation mode, the output of the digital acquisition system consists of the timestamps of neutrons interactions (e.g. captures times). These timestamps data have been processed by MATLAB scripts to construct arrays that contain the number of neutron counts over time bins. The results of this process are (approximately) equivalent to those from detectors operating in current mode. In current mode, detectors measure the neutron counts over time bins. The first part of this work summarizes the analytical and numerical frameworks to calculate the cross power spectral density. The second part discusses the conversion of the detector output data from timestamps to counts per time bin and shows the results obtained from the KUCA facility experimental data.

ANALYTICAL FRAMEWORK

It is assumed that a subcritical assembly is driven by an external pulsed neutron source operating in pulsed mode and that the pulse duration is small (e.g. from 5 to 100 μs) relative to the pulse repetition period t_r (e.g. from 10 to 50 ms). In addition, the assembly can be analyzed using the point kinetics approximation, delayed neutrons are at equilibrium during the detectors counting, and the detectors counting is an ergotic process. The latter assumption implies that the statistics of the counting rate of the detector does not change with time if the acquisition time of the detector signal is long enough (e.g. 10 accelerator pulses).

Within the above assumptions, the external neutron source as a function of time is given by Eq. 1 [1,2].

$$s(t) = s_0 \sum_{m=-\infty}^{+\infty} \delta(t - m t_r) \tag{1}$$

In Eq. 1, s_0 is the number of neutron released per pulse, m is an integer index, and δ is the Dirac delta function. The source as a function of frequency is given by the Fourier transform of Eq. 1, as shown in Eq. 2. Small letters are used for the functions of time t, whereas capital letters are used for the functions of frequency ω.

$$S(j\omega) = \int_{-\infty}^{+\infty} dt\, s(t) \exp(-j\omega t) = \\ = \frac{2\pi s_0}{t_r} \sum_{m=-\infty}^{+\infty} \delta(\omega - \omega_m) \tag{2}$$

In Eq. 2, ω_m is the angular repetition frequency defined in Eq. 3.

$$\omega_m \equiv \frac{2\pi m}{t_r} \tag{3}$$

The neutron population as a function of frequency is given by Eq. 4. The neutron population is averaged over the whole core due to the point kinetics assumption.

$$N(j\omega) = G(j\omega) S(j\omega) = \\ = \frac{2\pi s_0}{t_r} \sum_{m=-\infty}^{+\infty} \frac{\delta(\omega - \omega_m)}{\alpha_0 + j\omega} \tag{4}$$

In Eq. 4, α_0 is the prompt neutron decay constant (associated to the fundamental mode of the subcritical assembly), and $G(j\omega)$ is the zero-power reactor transfer function [3] on the frequency domain. The neutron population on the time domain is given by inverse Fourier transform of $N(j\omega)$, as shown in Eq. 5.

$$n(t) = \frac{1}{2\pi} \int_{-\infty}^{+\infty} d\omega\, N(j\omega) \exp(j\omega t) = \\ = \frac{s_0}{t_r} \sum_{m=-\infty}^{+\infty} \frac{\exp(j\omega_m t)}{\alpha_0 + j\omega_m} \tag{5}$$

Within this analytical framework, the cross-correlation function $\varphi(t_1, t_2)$ is defined as the ensemble average of two separate detectors counts, $c_a(t_1)$ and $c_b(t_2)$, as shown in Eq. 6. In Eq. 6, $c_a(t_a)$ and $c_b(t_b)$ are the average neutron counts at times t_a and t_b of detectors a and b, respectively. These detectors counts are averaged over a small arbitrary time bin dt.

$$\varphi(t_1, t_2) \equiv$$

$$\equiv \lim_{t_1 \to \infty} \frac{1}{t_1} \int_{-\infty}^{+t_1} dt_a \frac{1}{t_2 - t_1} \int_{+t_1}^{+t_2} dt_b c_a(t_a) c_b(t_b) \quad (6)$$

In Eq. 6, it is assumed that $t_2 > t_1$. For an ergotic process, Eq. 6 can be simplified to Eq. 7, by introducing the variable τ, defined as t_2-t_1 (Eq. 8).

$$\varphi(t_1, \tau) = \varphi(\tau) =$$

$$= \lim_{t_1 \to \infty} \frac{1}{t_1} \int_{-t_1/2}^{+t_1/2} dt_a \, c_a(t_a) c_b(\tau) \quad (7)$$

$$\tau \equiv t_2 - t_1 \quad (8)$$

For an ergotic process, the cross-correlation function is a function of only τ. It is assumed that the detectors counts *c* are proportional to the fission frequency λ_f, the neutron population *n*, and the detector efficiency ε, as shown in Eq. 9 for the detector *a* (an equal equation applies for the detector *b*).

$$c_a(t) \cong \lambda_f n(t) \varepsilon_a = \nu \Sigma_f n(t) \varepsilon_a \quad (9)$$

In Eq. 9, ν is the neutron velocity and Σ_f id the fission macroscopic cross section. It is assumed that once detector *a* counts a neutron from a fission chain, the detector b can eventually count ν-1 neutrons from the same (correlated) fission chain and ν neutrons from other (uncorrelated) fission chains (with ν being the number of fission neutrons per fission event).

The cross power spectral density $\Phi(\omega)$ is defined as the cross-correlation function on the frequency domain.

Within this analytical framework, Yamamoto [5] derived to the final formula for the cross power spectral density, written in Eq. 10.

$$\Phi(\omega) = \varepsilon_a \varepsilon_b \lambda_f \frac{s_0 \langle \nu(\nu - 1) \rangle}{\alpha_0 t_r (\alpha_0^2 + \omega^2)} - \varepsilon_a \varepsilon_b \frac{s_0}{t_r (\alpha_0^2 + \omega^2)} +$$

$$+ 2\pi \varepsilon_a \varepsilon_b \frac{s_0^2}{t_r^2} \sum_{m=-\infty}^{+\infty} \frac{\delta(\omega - \omega_m)}{(\alpha_0^2 + \omega_m^2)} \quad 10)$$

In Eq. 10, the brackets operator indicates the average over all fission events, the first term on the right-hand side relates to correlated fission chains, the third term on the right-hand side relates to uncorrelated fission chains, and the second term relates to correlated neutrons from a spallation event.

NUMERICAL FRAMEWORK

The numerical framework to calculate the cross power spectral density is illustrated in detail in Refs. [4, 5]. Assuming that the detectors counts are sampled over *M* (arbitrary) time bins, the circular correlation function R_{ab} is given by Eq. 11.

$$R_{ab}(n) \equiv \sum_{k=0}^{M-1} c_a(t_k) c_b\left(t_{M-(n-k)}\right);\ n \in \{1,2,\dots,M\} \quad (11)$$

In Eq. 11, $c_a(t_k)$ are the neutron counts of detector *a* within an arbitrary time bin Δt starting at time t_k. The real and imaginary parts of the cross power spectral density can be calculated using Eqs. 12 and 13, respectively.

$$Re\{\Phi(\omega_k\} = 2 \sum_{n=0}^{M-1} \left(R_{ab}(n) + R_{ba}(n)\right) \cos\left(\frac{2\pi k n}{M}\right) \quad (12)$$

$$Im\{\Phi(\omega_k\} = 2 \sum_{n=0}^{M-1} \left(R_{ba}(n) - R_{ab}(n)\right) \sin\left(\frac{2\pi k n}{M}\right) \quad (13)$$

In Eqs. 12 and 13, the integer index *k* extends from 0 to *M*/2 and ω_k is defined in Eq. 14.

$$\omega_k \equiv \frac{2\pi k}{\Delta t M}; \qquad k \in \left\{1,2,\dots,\frac{M}{2}\right\} \quad (14)$$

It is assumed that the term $\Delta t M$ appearing in Eq. 14 is much larger (e.g. 10 times) than the pulse repetition period t_r appearing in Eq. 3. If only the fundamental mode existed, the imaginary part of the cross power spectral density would be zero.

CALCULATION OF THE CROSS POWER SPECTRAL DENSITY FOR DETECTORS OPERATING IN PULSE MODE

Usually, detectors operate in current or pulse mode. In current mode, detectors measure the current induced by many ionization processes. In pulse mode, detectors measure the voltage induced by a single ionization process. For the current mode, the application of Eq. 11 is straightforward since the detectors counts are already averaged over the time bin Δt set by the digital acquisition system. In other words, the output of the digital acquisition system (when the detector operates in current mode) is the average neutron count over a time bin Δt. When detectors operate in pulse mode, the output of the digital acquisition system consists of the timestamps (e.g. the exact time when a neutron is captured) from each ionization process. The ionization process comes from neutron interaction with the detector material (e.g. B-10, He-3, or U-235). Consequently, when the detector operates in pulse mode, the detector counts must be converted from the "timestamps" format to "average" format. For a subcritical assembly driven by a

pulsed neutron source, this conversion can be accomplished by the following steps:

1) two arrays of 5,000 units are initialized to zero; the two arrays account for the neutron captures from 10 accelerator pulses (500 units per accelerator pulse) in detectors *a* and *b* separately (one array is c_a and the other is c_b);
2) each unit of the array represents the sum of neutron counts in a time interval Δt equal to the pulse repetition period t_r (e.g. 50 ms) divided by 500 (with 500 being an arbitrary large integer);
3) all the timestamps of the neutron captures in detectors *a* and *b* are read from the output file of the digital acquisition system and the two arrays are separately updated for detectors *a* and *b* to construct c_a and c_b.

Once the arrays c_a and c_b are constructed, the application of Eqs. 11 to 14 is straightforward and the retrieval of the prompt neutron decay constant is performed by a fitting process as discussed in detail in literature [1,2,5].

The first attempt to use timestamps for the construction of the auto power spectral density (which is defined when c_a and c_b come from a single detector instead of two separate detectors) has been performed by Kitamura et al. [6]. However, that methodology was implemented by programming the digital acquisition system, whereas the current work is based on MATLAB scripts without any modification of the digital acquisition system.

Finally, the cross power spectral density results obtained by detectors operating in current mode may differ from those obtained by detectors operating in pulse mode. This difference arises because, in current mode, the detector is not subjected to the dead-time effect; whereas, in pulse mode, some neutron counts are lost due to the dead-time effect. When the count rate is low (e.g. below 10,000 counts per second for a stationary source), dead-time effects are negligible.

RESULTS

The methodology discussed in the previous Sections, has been applied to the experimental results (in this work no neutron transport simulation has been performed) obtained from the KUCA facility of Japan [7,8]. The experimental data consist of timestamps recording the start of an accelerator pulse, the neutron captures in the BF_3 detector located at position U10, and the neutron captures in the fiber detector. In this experiment the pulse repetition period t_r is equal to 50 ms and the length of the experiment is approximately 12,000 accelerator pulses. The arrays c_a (neutron counts in the BF_3 detector located at position U10) and c_b (neutron counts in the fiber detector) have each 5,000 units and account for the all neutron counts in 10 pulses. More precisely the MATLAB script processing of the experimental data distributed all the neutron counts from 12,000 pulses to only 10 pulses. This post processing methodology is more flexible than the one applied by Kitamura et al. [6] since in this work the arbitrary time bin Δt and the arbitrary number of pulses for the construction of R_{ab} and R_{ba} can be changed. In contrast, the methodology of Kitamura et al. [6] is much less flexible since the change of the above arbitrary parameters (after the measurements are taken from the digital acquisition system) is not possible.

Figure 1 shows the arrays c_a and c_b, which account for the neutron counts in 10 accelerator pulses. These neutron counts refer to the KUCA configuration discussed in Ref. [7]. Figure 2 displays the circular correlation functions R_{ab} and R_{ba} constructed using Eq. 11 using the arrays c_a and c_b. In all parameters illustrated in Figs. 1 and 2, it is clearly visible that the accelerator pulses are delivered every 50 ms, which correspond to 500 units of the arrays.

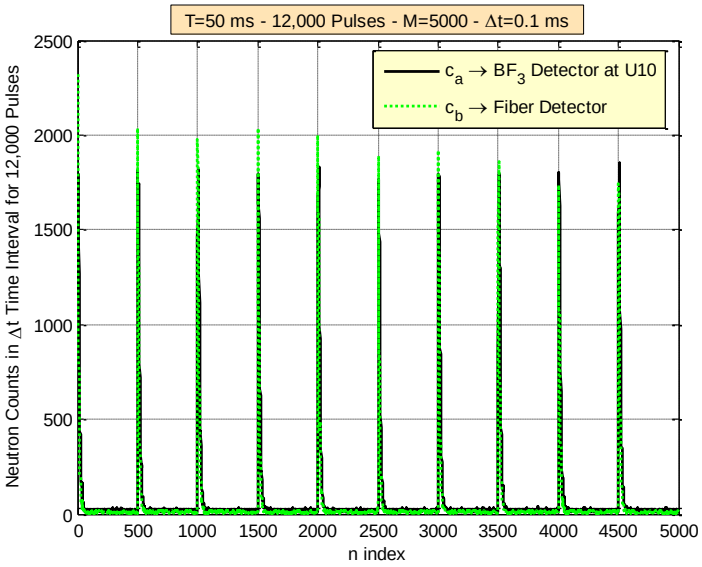

Fig. 1. Neutron counts arrays c_a and c_b.

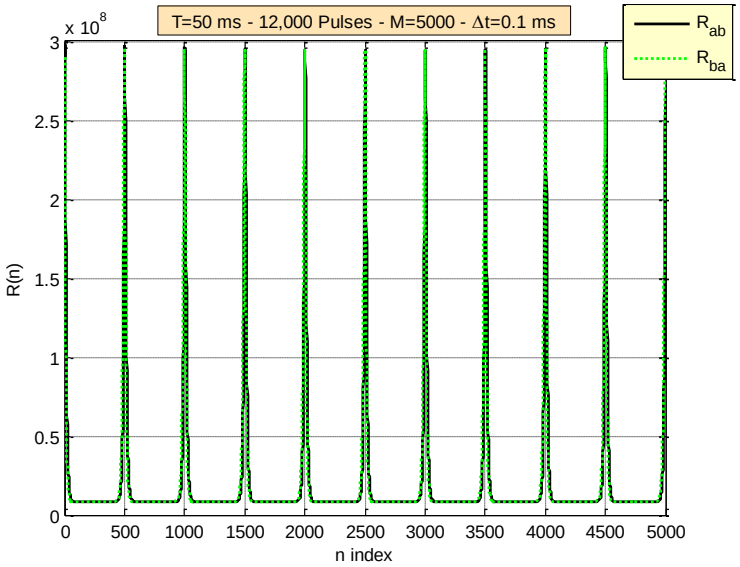

Fig. 2. Circular correlation functions R_{ab} and R_{ba}.

The real and imaginary parts of the cross power spectral density are illustrated in Fig. 3. The peaks of the real part relate to uncorrelated fission chains and allow to calculate the prompt neutron decay constant [1], as shown in Fig. 4. The fitting function to calculate the prompt neutron decay constant is given in Eq. 15.

$$Re\{\Phi(\omega)\} \cong \frac{A}{\alpha_0^2 + \omega^2} \qquad (15)$$

In Eq. 15, A is a constant given by the fitting procedure (which also gives α_0).

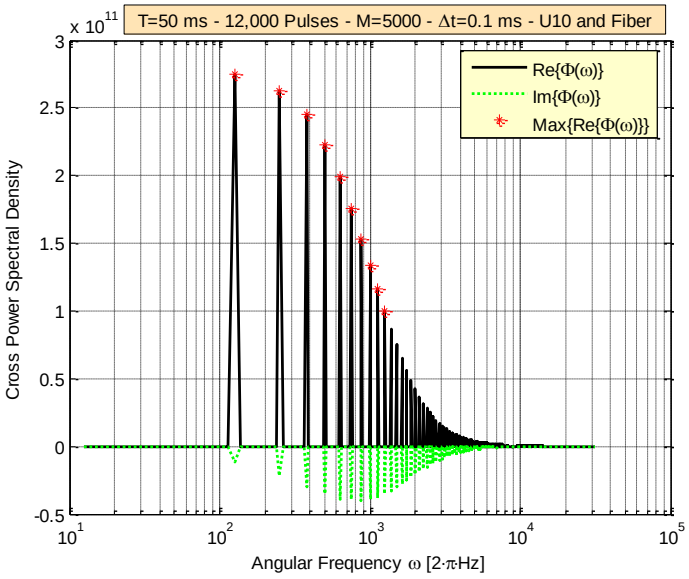

Fig. 3. Real and imaginary parts of the cross power spectral density as a function of the angular frequency (Eqs. 12 and 13).

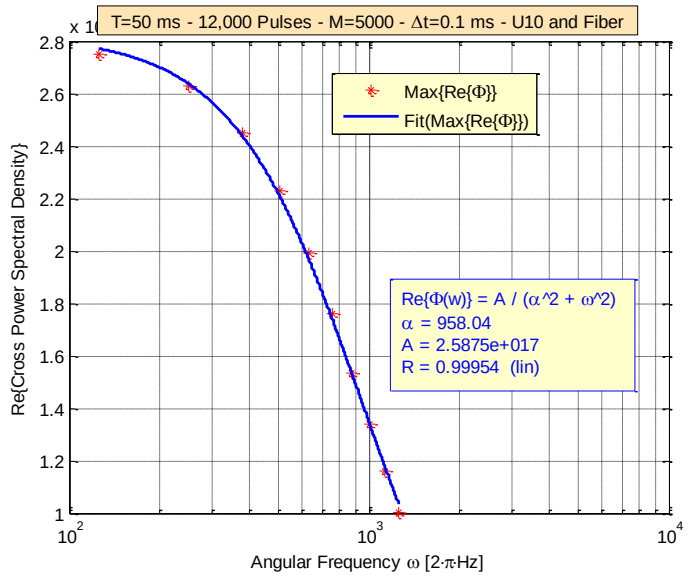

Fig. 4. Fitting the peaks of the (uncorrelated) real part of the cross power spectral density.

CONCLUSIONS

The value of the prompt neutron decay constant obtained from the cross power spectral density applied to the KUCA experimental data from detector operating in pulse mode is 958 1/s. This value is in good agreement with the one obtained from the slope of the neutron counts as a function of time for the BF_3 detector located at position U10 (964 1/s).

The non-zero imaginary part of the spectral neutron density indicates that higher order modes (in addition to the fundamental one) contribute to the neutron flux in the detectors. However, measuring the prompt neutron decay constant from two detectors located in different positions attenuates the special effects arising from the subcriticality of the experimental facility [9,10]. In addition, using two detectors eliminates the white noise (that is present in the auto power spectral density with only one detector).

The methodology presented in this work allows to change the arbitrary time bin Δt and the arbitrary number of pulses for the construction of circular correlation function after (not before and only once [6]) measurements are taken.

ACKNOWLEDGMENTS

This work is supported by the U.S. Department of Energy, Office of Material Management and Minimization (M3), National Nuclear Security Administration.

REFERENCES

[1] A. SAKON et al., "Power spectral analysis for a thermal subcritical reactor system driven by a pulsed 14 MeV neutron source," *Journal of Nuclear Science and Technology* ***50/5***, pp. 481-492 (2013).

[2] A. SAKON et al., "Measurement of large negative reactivity of an accelerator-driven system in the Kyoto University Critical Assembly," *Journal of Nuclear Science and Technology* ***51/1***, pp. 116-126 (2014).

[3] J.J. DUDERSTADT and L.J. HAMILTON, *Nuclear Reactor Analysis*, John Wiley and Sons, p. 253 (1976).

[4] T.E. VALENTINE and J.T. MIHALCZO, "MCNP-DSP: A neutron and gamma ray Monte carlo calculation of source-driven noise-measured parameters," *Annals of Nuclear Energy* ***23/16***, pp. 1271-1287 (1996).

[5] T. YAMAMOTO, "Frequency domain Monte Carlo simulation method for cross power spectral density driven by periodically pulsed spallation neutron source using complex-valued weight Monte Carlo," *Annals of Nuclear Energy* **63**, pp. 711-720 (2014).

[6] Y. KITAMURA et al., "Reactor Noise Experiments by Using Acquisition System for Time Series Data of

Pulse Train," *Journal of Nuclear Science and Technology* ***36/8***, pp. 653-660 (1999).

[7] A. TALAMO et al. "Advances in the computation of the Sjöstrand, Rossi, and Feynman distributions," *Progress in Nuclear Energy* ***101/C***, pp. 299-311 (2017).

[8] M. YAMANAKA et al. "Effective Delayed Neutron Fraction by Rossi-α Method in Accelerator-Driven System Experiments with 100 MeV Protons at Kyoto University Critical Assembly," *Journal of Nuclear Science and Technology*, **54/3**, pp. 293-300 (2017).

[9] A. TALAMO et al., "Correction Factor for the Experimental Prompt Neutron Decay Constant," *Annals of Nuclear Energy* ***62***, pp. 421-428 (2013).

[10] A. TALAMO et al., "Monte Carlo and Deterministic Calculation of the Bell and Glasstone Spatial Correction Factor," *Computer Physics Communications* ***183/9***, pp. 1904-1910 (2012).